IJARSCT
International Journal of Advanced Research in Science, Communication and Technology
International Open-Access, Double-Blind, Peer-Reviewed, Refereed, Multidisciplinary Online Journal
ISSN: 2581-9429
Volume 5, Issue 4, December 2025
Impact Factor: 7.67

A Study on the Joining Behavior Of Aluminium Alloys (Aa6061, Aa7075) and Aisi 304l Stainless Steel using Advanced Welding Techniques

Tarun Mittal
Lecturer, Department of Mechanical Engineering
Hindu College of Engineering, Sonipat

Abstract: *This present scholarly work of merit is studied from the perspective of the parametric effect on weld microstructural evolution and consequential mechanical properties alteration in precipitation-hardened aluminium (Al) AA6061-T6, AA7075-T651 and austenitic stainless steel (ASS) AISI 304L. The exploration of criticality and domain of weldability phenomena have been performed by adopting two advanced innovative joining technology; friction stir welding (FSW) and laser beam welding (LBW). Moderate strength AA6061-T6 and high strength AA7075-T651 are the most widely accepted alloys in many fabrication industries of commercial importance, particularly in different automobile, aerospace and military components industries. While ASS 304L are found with much diversified applications in thermal power plant, petrochemical, automotive, biomedical engineering and nuclear industries. On the other hand, being comparatively new technology, both FSW and LBW have gained wide recognitions among researchers and industries as a potentially powerful joining technology for aerospace, transportation, pipe joining and marine structural jobs. Going by the published research papers, it revealed that there have been difficulties for welding Al alloys by conventional welding such as gas tungsten arc welding (GTAW), gas metal arc welding (GMAW) processes, specifically precipitation-hardened AA6061 and AA7075 are facing defects related to solidification crack, distortion, porosity, micro-segregation and formation of brittle dendrite structure. There also revelation that the weldability of ASS can be challenging during conventional fusion welding process such as GTAW, GMAW due to higher possibility of sensitization, distortion and microstructural modification. Further, during joining of ASS with conventional welding, material softening at heat affected zone (HAZ) cannot be eradicated completely. So the proper selection of process implications could bring more integrity to the structural design. Bearing this in mind, the two novel techniques FSW and LBW have been tried to accomplish the structural joints for AA6061, AA7075 and AISI 304L*

Keywords*:* GTAW, GMAW, HAZ ASS 304L

I. INTRODUCTION

The high strength-to-weight ratio, good machinability and high resistance to corrosion are the governing properties of Al alloys which make it ideal as structural materials. Al alloys can broadly be separated into two major categories: non-heat-treatable and heat-treatable. The heat-treatable 6xxx and 7xxx systems are widely employed series [1]. Among the 6xxx and 7xxx systems, the AA6061-T6 and AA7075-T651 classes have gathered extensive acceptance in structural applications. The mechanical properties differ based on hardening-tempering process. Evidently, the two as-received test materials of Al alloy are designated with two different temper designations signifying different heat treatment paths. Even though, hardening treatment varies by industries, the typical solution and precipitation heat treatments of the T6 temper usually involve a solution treatment at 530ºC followed by quenching in water and then aging for 18 hours at around 160ºC. While, T651 hardening treatment includes a 480ºC solution heat treatment followed with stress relief by stretching. In a subsequent aging step, the alloy was precipitation heat treated at 120ºC for 24 hours. Mg in combinations with one or more of the elements, like; Si and Zn for 6061 and 7075 Al alloys, respectively speeds up and

IJARSCT
International Journal of Advanced Research in Science, Communication and Technology
International Open-Access, Double-Blind, Peer-Reviewed, Refereed, Multidisciplinary Online Journal
ISSN: 2581-9429 Volume 5, Issue 4, December 2025 Impact Factor: 7.67

accentuates the formation of strengthening precipitates. Thus, during the aging period, the strengthening precipitate Mg2Si (for AA6061-T6) and MgZn2 (for AA7075-T651) are evenly precipitated within the grains [2]. On the other hand, low carbon grade AISI 304L ASS is another experimental material of interest. This grade contains a maximum of 0.03% carbon in order to avoid the effect of complex carbide precipitation (M23C6: M=Cr/Fe/Mo) and minimize the possibility of Chromium depletion [3,4]. Moreover, the presence of such amount of carbon makes it a lower susceptible to corrosion [5]. Different advantageous inherent properties accompanied by low-pricing benefit have made the 304L a major work-horse in structural industries.

Naturally, in conformity with the international standard it becomes imperative to analyse the properties of commercially purchased as-received BM, so that, the weld joint quality relative to the corresponding BM may be evaluated precisely. In essence, this section aims to figure out the possible ways in which comparative studies can be pursued. This, in turn would enhance the reliability and acceptability of FSW and LBW in a greater sense.

II. RELATED WORK

Friction stir welding (FSW) has been widely adopted for joining high-strength aluminium alloys because it is a solid-state process that avoids the melting-related defects (porosity, hot cracking) associated with fusion welding. Guo (2014) provided an influential study of dissimilar FSW between AA6061 and AA7075, showing that material placement (which alloy is on the advancing side), tool geometry, and traverse/rotation speeds strongly affect material flow, nugget formation, and mechanical properties; optimal parameters produce coherent stir zones with improved tensile performance compared to poorly optimized runs.

Several experimental investigations corroborate the robustness of FSW for AA6061–AA7075 joints. Kaewkham et al. (2022) reported that careful selection of tool geometry and welding parameters can enhance microstructure uniformity and increase joint strength of dissimilar 6061/7075 FSW, while also noting the common formation of heterogeneous hardness profiles across the stir zones that require post-weld treatments for property homogenization.

FSW has also been applied to aluminum–steel couples, including AA6061 to stainless steels, though joining dissimilar Al–Fe systems introduces challenges due to intermetallic compound (IMC) formation and poor metallurgical compatibility. Newishy et al. (2023) demonstrated FSW of AA6061 to AISI 316, emphasizing process windows that minimize severe IMC layers and showing that mechanical interlocking and limited diffusion can yield serviceable dissimilar joints when process heat input is controlled. Mahto et al. (2019) further explored FSW of AA6061-T6 to AISI 304 in underwater FSW conditions, finding that the water medium alters cooling rates and can influence nugget morphology and residual stress but may reduce surface defects. These works indicate that FSW can produce acceptable Al–stainless joints when interfacial reactions are restricted by low heat input and optimized material placement.

By contrast, laser welding (a fusion technique) of AA7075 and similar high-strength aluminium alloys is more problematic because these alloys are prone to hot cracking and porosity during solidification. El-Batahgy et al. (2021) showed that high-power fiber laser welding with careful control of heat input and, where necessary, post-weld heat treatments or filler additions can partially recover mechanical properties of AA7075 welds, but solidification cracking remains a key concern. Alkhabbat et al. (2023) studied pulsed laser welding of AA7075 with different fillers and welding schedules and highlighted that choice of filler material and pulse parameters can mitigate solidification cracks and improve joint integrity. These findings emphasize that while laser welding can be viable for AA7075 under optimized conditions, it generally requires strict process control or filler usage to be successful.

Laser welding of stainless steels such as AISI 304L is well established; studies (e.g., Mahmoud 2021) have documented the process window mapping of laser power and speed to control fusion zone microstructure, HAZ, and mechanical response in 304L, with fiber and Nd:YAG lasers producing sound welds when parameters are optimized. However, when laser welding is applied to dissimilar Al–Fe combinations, differential melting and solidification behavior and extensive IMC formation make direct fusion joining difficult without interlayers or special techniques

III. MATERIALS AND METHODS

Commercially procured rolled sheets of AA6061-T6, AA7075-T651 with 3 mm thickness and AISI 304L of 2.5 mm thickness were used for the present investigation. Henceforth, these materials will be referred in the text as the base

IJARSCT
International Journal of Advanced Research in Science, Communication and Technology
International Open-Access, Double-Blind, Peer-Reviewed, Refereed, Multidisciplinary Online Journal
ISSN: 2581-9429 Volume 5, Issue 4, December 2025 Impact Factor: 7.67

materials (BM). The chemical composition of the as-received BM has been presented in Table 1. Chemical composition was determined using OES (Q4 TASMAN; BRUKER Corporation), incorporated with QMATRIX software. Microstructural features were examined by OM (DM2500 M integrated with LAS-V-4.12 Software; Leica Microsystems GmbH), FESEM (Merlin with EDAX-AMETEK; Carl Zeiss AG) and HRTEM (200KV, JEM-2100F; JEOL Ltd.). Specimens for microscopic examination were prepared by EDM sectioning and applying standard metallographic grinding and polishing techniques. The chemical etchant was Keller's reagent to expose the microstructure of the Al specimens, while aqua regia was used to etch the ASS specimen to reveal microstructure. The grain size measurement was performed by Image-J software using the linear intercept method. EBSD data acquisition has been carried out using Nordlys detector (Nordlys Max 2; Oxford Instruments, UK) fitted in FESEM (Auriga Compact; Carl Zeiss Microscope GmbH). The indexing and processing of acquired data were executed using Aztec HKL CHANNEL analysing software (Oxford Instruments, UK). In addition to the standard metallography polishing technique, a vibromet polisher was employed prior to EBSD data explorations. For TEM observation, a precision ion polishing system with a stereomicroscope (PIPS-691; Gatan Inc.) was used to produce electron-transparent thin foil. EDS was also employed for precipitate analysis in the TEM study. This study involved XRD diffractometer (Empyrean; Malvern PANalytical Ltd.) equipped with High Score plus software to analyse the phases of parent alloys in the present work. The Vickers microhardness (DFC420 VMHT; Leica Microsystems GmbH) profile (as per ASTM E-384:2006) was generated by measuring hardness along the middle of the transverse cross-section. A load of 500 gf and a dwell time of 15 seconds were adopted for the micro-hardness testing. The BM specimens were subjected to tensile testing to predict their mechanical properties; the tensile tests were performed in a tensile testing machine (5900R; Instron Structural Testing System, UK). The data acquisition and processing were done using Blue Hill-3 software. In addition, to identify precisely the mode of tensile fracture mechanism, the fractured surfaces were studied with the help of SEM (S-3400N; Hitachi Corporation) incorporated with INCA software.

Table 1 Nominal Chemical composition (wt%) of the as-received BMs.

	Materials		
Elements			
AA6061-T6		**AA7075-T651**	**AISI 304L**
C	-	-	0.02
Mg	1.03	2.11	-
Si	0.62	0.03	0.37
Zn	0.01	5.64	-
Cr	0.10	0.20	18.33
Ni	0.01	-	8.62
Cu	0.14	1.09	0.35
Mn	0.05	0.01	1.62
Mo	-	-	0.18
V	0.02	-	0.05
Nb	-	-	0.02
Ti	0.01	0.05	0.01
Co	-	-	0.08
N	-	-	0.06
Fe	0.31	0.11	Bal
Al	Bal.	Bal.	-

IV. RESULT & DISCUSSION

4.3.1 Tensile and Microhardness values

In Table 2 the important values like $\zeta_{Y.S}$, ζ_{UTS}, ε_u and n-values obtained from tensile tests performed on as received alloys of AA6061-T6, AA7075-T651 and 304L are summarized. A sign of anisotropy in the tensile mechanical

IJARSCT
International Journal of Advanced Research in Science, Communication and Technology
International Open-Access, Double-Blind, Peer-Reviewed, Refereed, Multidisciplinary Online Journal
ISSN: 2581-9429 Volume 5, Issue 4, December 2025 Impact Factor: 7.67

properties of all the BM specimens were observed. In every instance, the tensile test result of the specimen along TD was found to be less than that of results obtained from the other two directions. Hence, disregarding the alloy type the tensile strength result at TD is considered as the minimum characteristic strength property of BMs. The corresponding average engineering stress-strain response obtained from tensile tests at TD for each type of BM are displayed in Fig. 1a-c. Although, the $\zeta_{Y.S}$ and ζ_{UTS} of the AA6061-T6 are lower compared to AA7075-T651 BM but the ε_u is comparatively better. In regard to strength, AA7075-T651 is almost comparable to tested material 304L. Interestingly, the $\zeta_{Y.S}$ of 304L BM is registered in between the AA6061-T6 and AA7075-T651, while ε_u attains an impressively higher value.

Table 2 Summary of mechanical properties of as-received BMs measured at room temperature: (a) AA 6061-T6, (b) AA7075-T651 and (c) AISI 304L.

(a) AA6061-T6					
Orientation	**σY.S (MPa)**	**σUTS (MPa)**	**ε_u (%)**	**n- value**	**Hardness (HVN)**
RD	271.2	317.7	9.9	0.09	96±1
TD	248.1	293.1	8.9	0.09	
45° direction	265.4	307.8	7.2	0.08	
(b) AA7075-T651					
Orientation	**σY.S (MPa)**	**σUTS (MPa)**	**ε_u (%)**	**n-value**	**Hardness (HVN)**
RD	519.57	588.55	8.99	0.08	172±0.7
TD	502.42	566.56	8.73	0.07	
45° direction	510.51	581.23	8.81	0.07	
(c) AISI 304L					
Orientation	**σY.S (MPa)**	**σUTS (MPa)**	**ε_u (%)**	**n-value**	**Hardness (HVN)**
RD	318.17	675.3	59.77	0.21	186±2
TD	312.21	661.13	59.72	0.20	
45° direction	315.04	665.7	59.25	0.21	

Table 2 also presents the hardness value of as-received BMs. To maintain the parity with welded specimens, the hardness of the BM were measured across the TD and along mid-section on thickness. The lowest hardness value was observed for AA6061 BM. It is noted that the hardness of AA7075 BM is comparable with the 304L BM. The diversified mechanical properties of Al alloys are related to the tempering process induced precipitation characteristics. Additionally, the existence of relatively higher amount of Mg and Cu in AA7075 BM, form the basis of marked increase in strength and hardness by solid-solution strengthening and precipitation hardening mechanism. On the contrary, high hardness and strength combined with wonderful ductility are chiefly achieved through cold working. Even though initial strength of 304L alloy depends upon the alloy composition, the improved mechanical properties can be reasonably related to cold working [5-9].

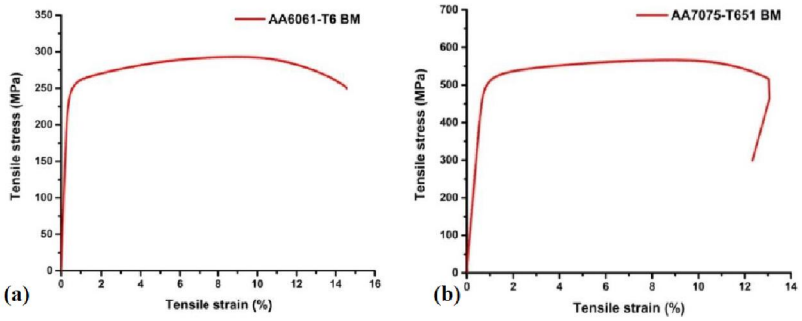

IJARSCT
International Journal of Advanced Research in Science, Communication and Technology
International Open-Access, Double-Blind, Peer-Reviewed, Refereed, Multidisciplinary Online Journal
ISSN: 2581-9429
Volume 5, Issue 4, December 2025
Impact Factor: 7.67

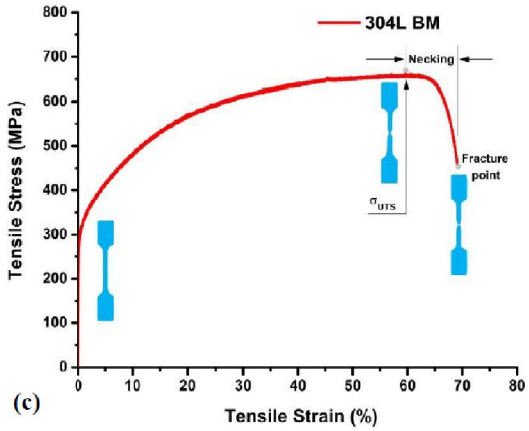

Fig. 1. Engineering stress-strain curve at TD orientation (minimum tensile properties) of as received BM: (a) AA6061-T6 (b) AA7075-T651 (c) AISI 304L.

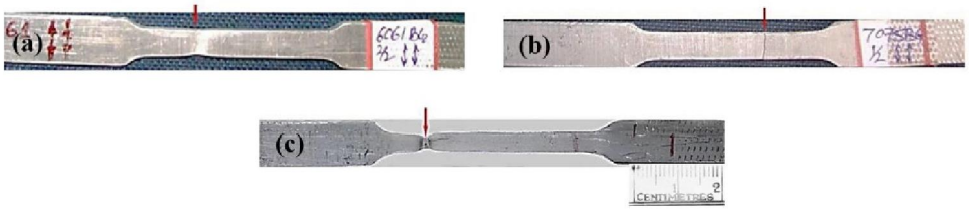

Fig. 2. Snapshot of characteristic necking feature for as received BM specimens at TD orientation: (a) AA6061-T6 (b) AA7075-T651 and (c) AISI 304L.

equiaxed dimples accompanied by predominant fibrous features throughout the fractured surface; typical behaviour of ductile materials and a strong indication of microscopic plasticity which substantiates the fact of extremely large elongation (Fig. 3c) [10, 11]. However, the further knowledge of microstructural manifestation is required to be documented to correlate the subtle microstructure-mechanical property interrelation of these alloys.

4.3.3 Microstructural Characterization

4.3.3.1 Phase analysis

From the XRD patterns of individual Al alloy (Fig. 4a and Fig. 4b) existence of the hardening precipitates Mg2Si (for AA6061-T6) and MgZn2 (for AA7075-T651) have been confirmed. In addition both the Al specimens contain Cu rich (AlCu, Al2CuMg) particles in Al metal matrix. On the other hand, XRD diffractogram of 304L BM (Fig. 4c) revealed the presence of δ-phase in characteristic γ-phase matrix.

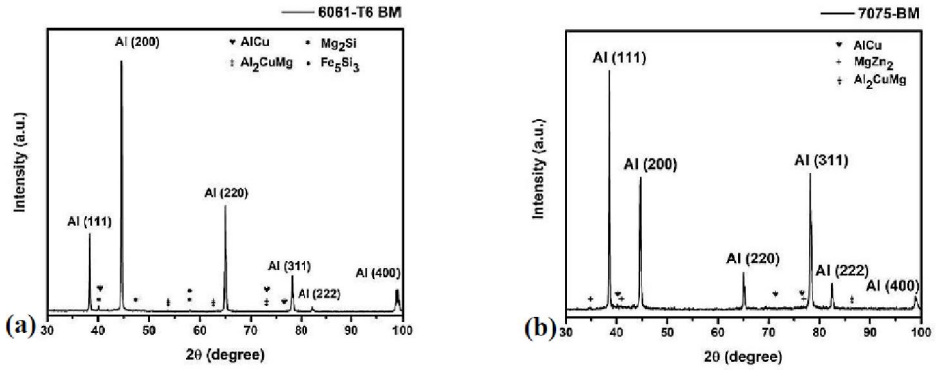

IJARSCT
International Journal of Advanced Research in Science, Communication and Technology
International Open-Access, Double-Blind, Peer-Reviewed, Refereed, Multidisciplinary Online Journal
ISSN: 2581-9429
Volume 5, Issue 4, December 2025
Impact Factor: 7.67

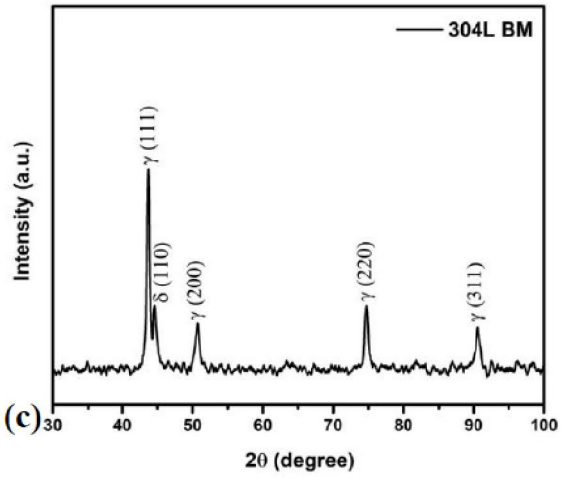

Fig. 4. XRD pattern demonstrating different phases for as received BM specimen: (a) AA6061-T6 (b) AA7075-T651 and (c) AISI 304L

4.3.3.2 OM and FESEM analysis

With the help of different images in Fig. 5 and Fig. 6, the discernible microstructural features of as-received BMs can easily be differentiated. The microstructure of AA6061 contains mostly elongated grains with a blend of cellular-shaped grains having average grain size 47.3±2.5 µm (Fig. 5a). Fig. 6a and Fig. 7a also exhibit virtually spherical shaped Mg and Si rich second phase intergranular segregations indicating the presence of strengthening phase Mg2Si. Additionally, there is indiscriminate dispersion of AlxMgy intra-granular phases (Fig. 7b).

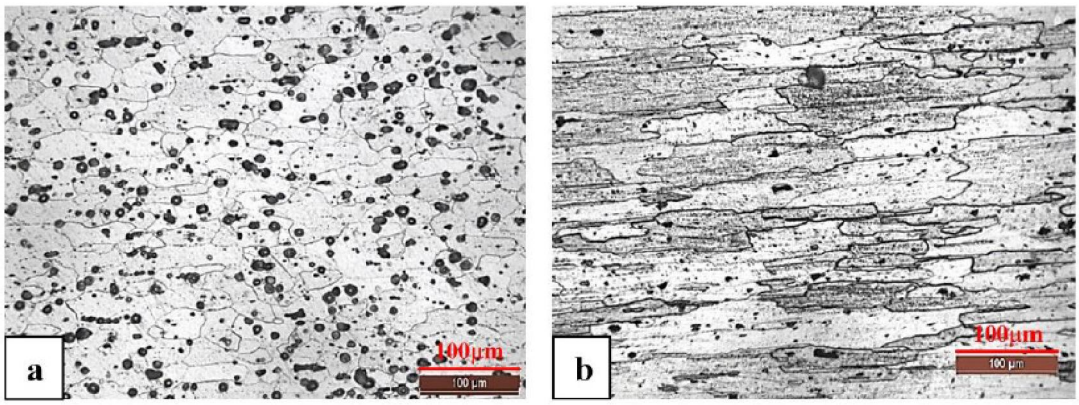

IJARSCT
International Journal of Advanced Research in Science, Communication and Technology
International Open-Access, Double-Blind, Peer-Reviewed, Refereed, Multidisciplinary Online Journal
ISSN: 2581-9429
Volume 5, Issue 4, December 2025
Impact Factor: 7.67

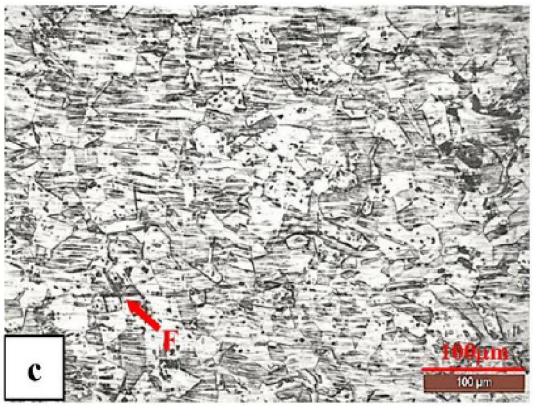

Fig. 5. Optical micrographs of transverse cross-section of different as-received BM showing different grain feature: (a) AA6061-T6 (b) AA7075-T651 (c) AISI 304L. F: ferrite.

In contrast, AA7075 BM is clearly found with irregularly large elongated pancake shaped grains; typical for a rolled and subsequently T651 tempered structure (Fig. 5b and Fig. 6b). The grain size is measured □149 ± 10 µm in the TD and ~20±2 µm wide in the ND. Fine insoluble second phase of about 1.2 to 17.6 µm size could be found as dispersed intergranular and intra-granularly. As can be observed from Fig. 5c and Fig. 5d, these scattered secondary phases are rich in Mg, Zn, Cu and Fe. Overall microscopy of tested Al alloys exhibit clearer feature of microstructure variance in addition to different size and distribution of constituent particles. These particles might have influence against the coarsening of the grains by pinning the grain boundaries.

A totally different microstructural feature having average grain size of □28.57 µm ± 2.96 was observed for 304L BM. The specimen displayed of polygonal austenite grain structures in conjunction with high fraction of annealing twins interspersed in several grains. It is reported that, due to its low SFE, static recrystallization and grain growth during heat treatment cause these twins [12-13]. Specimen also reveals a banded microstructure caused by the rolling deformation. Moreover, stringers of δ-phase can be seen in the microstructure. The grain boundary phases as found were essentially rich in Cr and Mn . During the non-equilibrium rapid solidification condition, the high cooling rate may result incomplete ferrite to austenite transformation and some δ-phase may be remained unavoidably in the solidified structure [13-14].

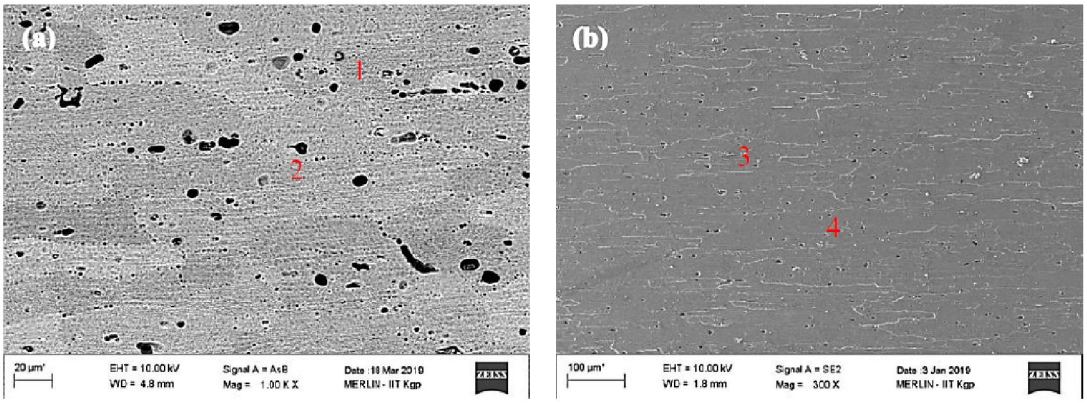

DOI: 10.48175/568

IJARSCT
International Journal of Advanced Research in Science, Communication and Technology
International Open-Access, Double-Blind, Peer-Reviewed, Refereed, Multidisciplinary Online Journal
ISSN: 2581-9429
Volume 5, Issue 4, December 2025
Impact Factor: 7.67

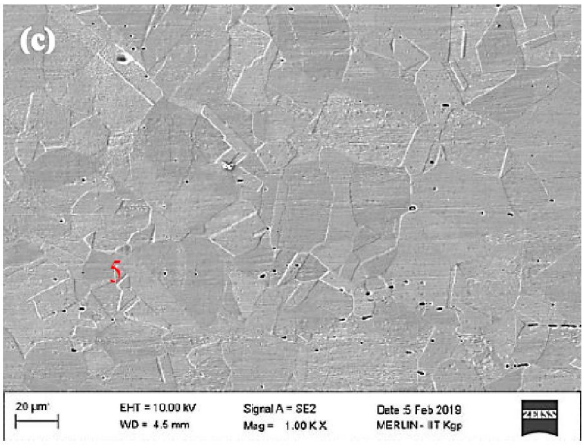

Fig. 6. FESEM micrographs of different as-received BM showing different morphology: (a) AA6061-T6 (b) AA7075-T651 (c) AISI 304L.

V. CONCLUSION

Results and discussion indicate all the investigated microstructures have gained considerable recovery from the rolled condition. Moreover, the mechanical properties of the investigated Al alloys 6061-T6 and 7075-T651 have been reasonably related with the morphology, volume fraction of strengthening precipitates and their interaction with dislocations. On the other hand, the main reason behind the distinct mechanical properties of 304L BM is credited to the mutual and interactive behavioural activities of dislocations with twinning, slip system and SFs. This chapter thus manifests that these commercially procured materials are in metallurgically and mechanically compliance with the global standard.

REFERENCES

[1] Y. Guo, "Dissimilar friction stir welding between AA6061 and AA7075 aluminum alloys: influence of process parameters on microstructure and mechanical properties," *Materials & Design*, vol. 64, pp. 619–628, 2014.
[2] S. Kaewkham, P. Thong-on, and C. Nookuea, "Microstructural evolution and mechanical properties of dissimilar AA6061–AA7075 joints fabricated by friction stir welding," *Journal of Manufacturing Processes*, vol. 78, pp. 105–118, 2022.
[3] A. Newishy, M. A. Seliem, and A. M. El-Shennawy, "Investigation of friction stir welding process parameters on the interfacial microstructure of AA6061–AISI 316 dissimilar joints," *Journal of Materials Research and Technology*, vol. 24, pp. 3512–3524, 2023.
[4] R. Mahto, P. Biswas, and P. Sahoo, "Underwater friction stir welding of dissimilar AA6061-T6 and AISI 304: effect on microstructure and mechanical properties," *Journal of Materials Engineering and Performance*, vol. 28, no. 9, pp. 5896–5908, 2019.
[5] H. El-Batahgy, M. M. F. Darwish, and M. M. Taha, "Optimization of fiber laser welding of AA7075 aluminum alloy for improved mechanical performance," *Optics & Laser Technology*, vol. 143, p. 107390, 2021.
[6] A. Alkhabbat, M. N. Abbas, and S. K. A. Rahim, "Influence of filler composition and pulse parameters on the microstructure and mechanical properties of pulsed laser welded AA7075 aluminum alloy," *Metals*, vol. 13, no. 4, p. 712, 2023.
[7] A. Mahmoud, "Laser welding of AISI 304L stainless steel: process optimization and microstructural characterization," *Journal of Materials Processing Technology*, vol. 298, p. 117297, 2021.
[8] R. Balasubramanian and V. Jayakumar, "Microstructure and mechanical characterization of AA6061-T6 aluminum alloy under T6 and T651 temper conditions," *Materials Characterization*, vol. 154, pp. 93–101, 2019.

IJARSCT
International Journal of Advanced Research in Science, Communication and Technology
International Open-Access, Double-Blind, Peer-Reviewed, Refereed, Multidisciplinary Online Journal
ISSN: 2581-9429 Volume 5, Issue 4, December 2025 Impact Factor: 7.67

[9] J. Zhang, X. Liu, and D. Zhang, "Effect of aging treatment on precipitation behavior and mechanical properties of AA7075 aluminum alloy," *Transactions of Nonferrous Metals Society of China*, vol. 30, no. 3, pp. 612–622, 2020.
[10] P. K. Pal, S. R. Maity, and D. Chakraborty, "Comparative analysis of microstructure and mechanical properties of AA6061 and AA7075 aluminum alloys," *Procedia Manufacturing*, vol. 30, pp. 671–678, 2019.
[11] R. Singh, A. Raturi, and S. Kumar, "Evaluation of microstructure, corrosion, and mechanical properties of AISI 304L stainless steel," *Journal of Materials Science: Materials in Engineering*, vol. 32, pp. 4201–4214, 2021.
[12] M. A. Shaikh and T. Watanabe, "Formation of intermetallic compounds during dissimilar welding of aluminum to stainless steel," *Materials Transactions*, vol. 59, no. 1, pp. 32–41, 2018.
[13] D. W. Zhang and Y. H. Zhao, "Microstructure and mechanical behavior of friction stir welded AA6061 and AISI 304L joints," *Materials Science and Engineering A*, vol. 758, pp. 92–102, 2019.
[14] H. Wang, L. Liu, and J. Chen, "Characterization of fiber laser welding of aluminum alloys and stainless steels using nickel-based interlayers," *Optics and Lasers in Engineering*, vol. 136, p. 106285, 2021.
[15] ASTM E384–17, *Standard Test Method for Microindentation Hardness of Materials*, ASTM International, West Conshohocken, PA, USA, 2017.
[16] S. R. Reddy, P. K. Gupta, and S. K. Singh, "Study on precipitation strengthening in aluminum alloys: Mg2Si and MgZn2 phase evolution," *Materials Today: Proceedings*, vol. 46, pp. 8571–8579, 2021.
[17] S. R. Chen, T. H. Lee, and M. S. Park, "Microstructural evolution and annealing twin formation in AISI 304L stainless steel," *Metallurgical and Materials Transactions A*, vol. 52, pp. 4228–4239, 2021.
[18] H. Luo, J. Sun, and P. K. Liaw, "Deformation mechanisms and twinning behavior in low stacking fault energy austenitic stainless steels," *Acta Materialia*, vol. 194, pp. 444–458, 2020.
[19] R. Mishra and Z. Ma, "Friction stir welding and processing," *Materials Science and Engineering: R: Reports*, vol. 50, no. 1–2, pp. 1–78, 2005.
[20] J. Hirsch and T. Al-Samman, "Superior light metals by texture engineering: optimized aluminum and magnesium alloys for automotive applications," *Acta Materialia*, vol. 61, no. 3, pp. 818–843, 2013